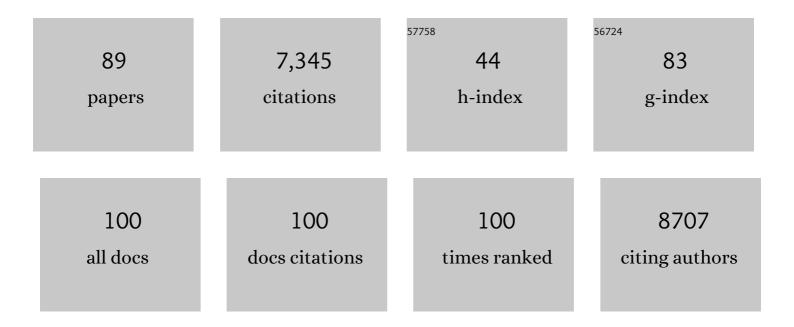
List of Publications by Year in descending order

Source: https://exaly.com/author-pdf/138214/publications.pdf Version: 2024-02-01



KE ZHANC

1 Recent dec 2010, 467,	ine in the global land evapotranspiration trend due to limited moisture supply. Nature,		
2010, 107,	951-954.	27.8	1,771
	us satelliteâ€derived global record of land surface evapotranspiration from 1983 to 2006. urces Research, 2010, 46, .	4.2	444
A review of Reviews: W	remote sensing based actual evapotranspiration estimation. Wiley Interdisciplinary ater, 2016, 3, 834-853.	6.5	380
	the Arctic System for Freshwater Cycle Intensification: Observations and Expectations. limate, 2010, 23, 5715-5737.	3.2	303
5 Vegetation 5 Evapotrans	Greening and Climate Change Promote Multidecadal Rises of Global Land piration. Scientific Reports, 2015, 5, 15956.	3.3	265
6 Satellite ba from 1983	sed analysis of northern ET trends and associated changes in the regional water balance to 2005. Journal of Hydrology, 2009, 379, 92-110.	5.4	212
7 Geographic 7 Journal of F	ally weighted regression based methods for merging satellite and gauge precipitation. ydrology, 2018, 558, 275-289.	5.4	181
	heterogeneity determines the ecological resilience of the Amazon to climate change. s of the National Academy of Sciences of the United States of America, 2016, 113, 793-797.	7.1	161
9 Increased c 356-362.	ontrol of vegetation on global terrestrial energy fluxes. Nature Climate Change, 2020, 10,	18.8	152
	noff generation modelling framework based on spatial combination of three runoff schemes for semi-humid and semi-arid watersheds. Journal of Hydrology, 2020, 590, 125440.	5.4	120
11 Characteris Shaanxi Pro	tics and influencing factors of rainfall-induced landslide and debris flow hazards in vince, China. Natural Hazards and Earth System Sciences, 2019, 19, 93-105.	3.6	119
12 <scp>A<td>stem mortality rates determines patterns of aboveâ€ground biomass in p>mazonian forests: implications for dynamic global vegetation models. Global Change 16, 22, 3996-4013.</td><td>9.5</td><td>116</td></scp>	stem mortality rates determines patterns of aboveâ€ground biomass in p>mazonian forests: implications for dynamic global vegetation models. Global Change 16, 22, 3996-4013.	9.5	116
Changes in	precipitation extremes in the Yangtze River Basin during 1960–2019 and the association warming, ENSO, and local effects. Science of the Total Environment, 2021, 760, 144244.	8.0	113
14 Trends in e upper reac	apotranspiration and their responses to climate change and vegetation greening over the les of the Yellow River Basin. Agricultural and Forest Meteorology, 2018, 263, 118-129.	4.8	111
15 Moisture: A	vity of North American Terrestrial Carbon Fluxes to Spatial and Temporal Variation in Soil n Analysis Using Radarâ€Đerived Estimates of Rootâ€Zone Soil Moisture. Journal of l Research G: Biogeosciences, 2019, 124, 3208-3231.	3.0	111
Ground ob	ervation-based analysis of soil moisture spatiotemporal variability across a humid to transitional zone in China. Journal of Hydrology, 2019, 574, 903-914.	5.4	104
	ased model detection of recent climateâ€driven changes in northern highâ€latitude vegetation ⁄. Journal of Geophysical Research, 2008, 113, .	3.3	99
	Amazonian ecosystems over the coming century arising from changes in climate, c <scp>CO</scp> _{2,} and land use. Global Change Biology, 2015, 21, 2569-2587.	9.5	97

#	Article	IF	CITATIONS
19	Improving the flood prediction capability of the Xinanjiang model in ungauged nested catchments by coupling it with the geomorphologic instantaneous unit hydrograph. Journal of Hydrology, 2014, 517, 1035-1048.	5.4	94
20	Northern highâ€latitude ecosystems respond to climate change. Eos, 2007, 88, 333-335.	0.1	92
21	Analysis of flash flood disaster characteristics in China from 2011 to 2015. Natural Hazards, 2018, 90, 407-420.	3.4	92
22	Satellite Microwave Remote Sensing of Daily Land Surface Air Temperature Minima and Maxima From AMSR-E. IEEE Journal of Selected Topics in Applied Earth Observations and Remote Sensing, 2010, 3, 111-123.	4.9	91
23	Physically-based landslide prediction over a large region: Scaling low-resolution hydrological model results for high-resolution slope stability assessment. Environmental Modelling and Software, 2020, 124, 104607.	4.5	87
24	Water balanceâ€based actual evapotranspiration reconstruction from ground and satellite observations over the conterminous <scp>U</scp> nited <scp>S</scp> tates. Water Resources Research, 2015, 51, 6485-6499.	4.2	79
25	Impacts of future deforestation and climate change on the hydrology of the Amazon Basin: a multi-model analysis with a new set of land-cover change scenarios. Hydrology and Earth System Sciences, 2017, 21, 1455-1475.	4.9	69
26	A comprehensive assessment framework for quantifying climatic and anthropogenic contributions to streamflow changes: A case study in a typical semi-arid North China basin. Environmental Modelling and Software, 2020, 128, 104704.	4.5	69
27	A priori parameter estimates for a distributed, grid-based Xinanjiang model using geographically based information. Journal of Hydrology, 2012, 468-469, 47-62.	5.4	67
28	Sensitivity of hydrological models to temporal and spatial resolutions of rainfall data. Hydrology and Earth System Sciences, 2019, 23, 2647-2663.	4.9	66
29	Exploring the utility of radar and satellite-sensed precipitation and their dynamic bias correction for integrated prediction of flood and landslide hazards. Journal of Hydrology, 2021, 603, 126964.	5.4	66
30	Coupling the k-nearest neighbor procedure with the Kalman filter for real-time updating of the hydraulic model in flood forecasting. International Journal of Sediment Research, 2016, 31, 149-158.	3.5	65
31	An integrated flood risk assessment approach based on coupled hydrological-hydraulic modeling and bottom-up hazard vulnerability analysis. Environmental Modelling and Software, 2022, 148, 105279.	4.5	65
32	Ecosystem heterogeneity and diversity mitigate Amazon forest resilience to frequent extreme droughts. New Phytologist, 2018, 219, 914-931.	7.3	64
33	Changing freezeâ€ŧhaw seasons in northern high latitudes and associated influences on evapotranspiration. Hydrological Processes, 2011, 25, 4142-4151.	2.6	62
34	The biophysics, ecology, and biogeochemistry of functionally diverse, vertically and horizontally heterogeneous ecosystems: the Ecosystem Demography model, version 2.2 – Part 1: Model description. Geoscientific Model Development, 2019, 12, 4309-4346.	3.6	62
35	A Satellite Approach to Estimate Land–Atmosphere \$hbox{CO}_{2}\$ Exchange for Boreal and Arctic Biomes Using MODIS and AMSR-E. IEEE Transactions on Geoscience and Remote Sensing, 2009, 47, 569-587.	6.3	58
36	Spatiotemporal characteristics and attribution of dry/wet conditions in the Weihe River Basin within a typical monsoon transition zone of East Asia over the recent 547 years. Environmental Modelling and Software, 2021, 143, 105116.	4.5	58

#	Article	IF	CITATIONS
37	A Comprehensive Evaluation of Five Evapotranspiration Datasets Based on Ground and GRACE Satellite Observations: Implications for Improvement of Evapotranspiration Retrieval Algorithm. Remote Sensing, 2021, 13, 2414.	4.0	54
38	Evaluation of the TRMM multisatellite precipitation analysis and its applicability in supporting reservoir operation and water resources management in Hanjiang basin, China. Journal of Hydrology, 2017, 549, 313-325.	5.4	52
39	Comparison of Three GIS-Based Hydrological Models. Journal of Hydrologic Engineering - ASCE, 2008, 13, 364-370.	1.9	50
40	Sensitivity of inferred climate model skill to evaluation decisions: a case study using CMIP5 evapotranspiration. Environmental Research Letters, 2013, 8, 024028.	5.2	50
41	Using multi-satellite microwave remote sensing observations for retrieval of daily surface soil moisture across China. Water Science and Engineering, 2019, 12, 85-97.	3.2	49
42	Multiple hydrological models comparison and an improved Bayesian model averaging approach for ensemble prediction over semi-humid regions. Stochastic Environmental Research and Risk Assessment, 2019, 33, 217-238.	4.0	48
43	iCRESTRIGRS: a coupled modeling system for cascading flood–landslide disaster forecasting. Hydrology and Earth System Sciences, 2016, 20, 5035-5048.	4.9	47
44	New Multisite Cascading Calibration Approach for Hydrological Models: Case Study in the Red River Basin Using the VIC Model. Journal of Hydrologic Engineering - ASCE, 2016, 21, .	1.9	47
45	Development of a coupled hydrological-geotechnical framework for rainfall-induced landslides prediction. Journal of Hydrology, 2016, 543, 395-405.	5.4	46
46	Refining a Distributed Linear Reservoir Routing Method to Improve Performance of the CREST Model. Journal of Hydrologic Engineering - ASCE, 2017, 22, .	1.9	44
47	Flood hazard mapping and assessment in data-scarce Nyaungdon area, Myanmar. PLoS ONE, 2019, 14, e0224558.	2.5	44
48	Changing Amazon biomass and the role of atmospheric CO ₂ concentration, climate, and land use. Global Biogeochemical Cycles, 2016, 30, 18-39.	4.9	32
49	Land cover change explains the increasing discharge of the Paraná River. Regional Environmental Change, 2018, 18, 1871-1881.	2.9	32
50	Applicability assessment of the CASCade Two Dimensional SEDiment (CASC2Dâ€ S ED) distributed hydrological model for flood forecasting across four typical medium and small watersheds in China. Journal of Flood Risk Management, 2019, 12, .	3.3	32
51	Analysis and Projection of Land-Use/Land-Cover Dynamics through Scenario-Based Simulations Using the CA-Markov Model: A Case Study in Guanting Reservoir Basin, China. Sustainability, 2020, 12, 3747.	3.2	32
52	Simulating canopy conductance of the Haloxylon ammodendron shrubland in an arid inland river basin of northwest China. Agricultural and Forest Meteorology, 2018, 249, 22-34.	4.8	31
53	Application and Sensitivity Analysis of Artificial Neural Network for Prediction of Chemical Oxygen Demand. Water Resources Management, 2018, 32, 273-283.	3.9	30
54	GA-PIC: An improved Green-Ampt rainfall-runoff model with a physically based infiltration distribution curve for semi-arid basins. Journal of Hydrology, 2020, 586, 124900.	5.4	30

#	Article	IF	CITATIONS
55	Improving flood simulation capability of the WRF-Hydro-RAPID model using a multi-source precipitation merging method. Journal of Hydrology, 2021, 592, 125814.	5.4	30
56	Analysis of drought and vulnerability in the North Darfur region of Sudan. Land Degradation and Development, 2018, 29, 4424-4438.	3.9	29
57	The biophysics, ecology, and biogeochemistry of functionally diverse, vertically and horizontally heterogeneous ecosystems: the Ecosystem Demography model, version 2.2 – Part 2: Model evaluation for tropical South America. Geoscientific Model Development, 2019, 12, 4347-4374.	3.6	29
58	Impacts of largeâ€scale oscillations on panâ€Arctic terrestrial net primary production. Geophysical Research Letters, 2007, 34, .	4.0	27
59	A comprehensive flash flood defense system in China: overview, achievements, and outlook. Natural Hazards, 2018, 92, 727-740.	3.4	26
60	A probabilistic method for streamflow projection and associated uncertainty analysis in a data sparse alpine region. Global and Planetary Change, 2018, 165, 100-113.	3.5	26
61	Evaluation of flood prediction capability of the distributed Gridâ€Xinanjiang model driven by weather research and forecasting precipitation. Journal of Flood Risk Management, 2019, 12, .	3.3	24
62	Sensitivity of pan-Arctic terrestrial net primary productivity simulations to daily surface meteorology from NCEP-NCAR and ERA-40 reanalyses. Journal of Geophysical Research, 2007, 112, .	3.3	23
63	Large-scale climate patterns and precipitation in an arid endorheic region: linkage and underlying mechanism. Environmental Research Letters, 2016, 11, 044006.	5.2	20
64	Bias orrected data sets of climate model outputs at uniform space–time resolution for land surface modelling over Amazonia. International Journal of Climatology, 2017, 37, 621-636.	3.5	17
65	Application of a developed distributed hydrological model based on the mixed runoff generation model and 2D kinematic wave flow routing model for better flood forecasting. Atmospheric Science Letters, 2017, 18, 284-293.	1.9	17
66	Improving the flood prediction capability of the Xin'anjiang model by formulating a new physics-based routing framework and a key routing parameter estimation method. Journal of Hydrology, 2021, 603, 126867.	5.4	17
67	Spatiotemporal changes of precipitation extremes in Bangladesh during 1987–2017 and their connections with climate changes, climate oscillations, and monsoon dynamics. Global and Planetary Change, 2022, 208, 103712.	3.5	17
68	Evaluation of Flood Prediction Capability of the WRF-Hydro Model Based on Multiple Forcing Scenarios. Water (Switzerland), 2020, 12, 874.	2.7	16
69	Projections of Future Climate Change in Singapore Based on a Multi-Site Multivariate Downscaling Approach. Water (Switzerland), 2019, 11, 2300.	2.7	15
70	Climatology and changes in hourly precipitation extremes over China during 1970–2018. Science of the Total Environment, 2022, 839, 156297.	8.0	13
71	Characteristics of Urban Waterlogging and Flash Flood Hazards and Their Integrated Preventive Measures: Case Study in Fuzhou, China. Journal of Sustainable Water in the Built Environment, 2018, 4,	1.6	11
72	Quantifying natural recharge characteristics of shallow aquifers in groundwater overexploitation zone of North China. Water Science and Engineering, 2021, 14, 184-192.	3.2	11

#	Article	IF	CITATIONS
73	GDBC: A tool for generating global-scale distributed basin morphometry. Environmental Modelling and Software, 2016, 83, 212-223.	4.5	10
74	Application and comparison of coaxial correlation diagram and hydrological model for reconstructing flood series under human disturbance. Journal of Mountain Science, 2016, 13, 1245-1264.	2.0	10
75	Applying a statistical method to streamflow reduction caused by underground mining for coal in the Kuye River basin. Science China Technological Sciences, 2016, 59, 1911-1920.	4.0	8
76	Estimation of Active Stream Network Length in a Hilly Headwater Catchment Using Recession Flow Analysis. Water (Switzerland), 2017, 9, 348.	2.7	6
77	Predictability of a Physically Based Model for Rainfall-induced Shallow Landslides: Model Development and Case Studies. , 2015, , 165-178.		6
78	Runoff sensitivity over Asia: Role of climate variables and initial soil conditions. Journal of Geophysical Research D: Atmospheres, 2017, 122, 2218-2238.	3.3	4
79	A New Runoff Routing Scheme for Xin'anjiang Model and Its Routing Parameters Estimation Based on Geographical Information. Water (Switzerland), 2020, 12, 3429.	2.7	4
80	Evaluating performance dependency of a geomorphologic instantaneous unit hydrograph-based hydrological model on DEM resolution. Water Science and Engineering, 2022, 15, 179-188.	3.2	4
81	On simulation improvement of the <scp>N</scp> oah_ <scp>LSM</scp> by coupling with a hydrological model using a doubleâ€excess runoff production scheme in the <scp>GRAPES</scp> _ <scp>M</scp> eso model. Meteorological Applications, 2017, 24, 512-520.	2.1	3
82	Evaporation Processes and Changes Over the Northern Regions. , 2021, , 101-131.		2
83	Assimilation of surface soil moisture jointly retrieved by multiple microwave satellites into the WRF-Hydro model in ungauged regions: Towards a robust flood simulation and forecasting. Environmental Modelling and Software, 2022, 154, 105421.	4.5	2
84	Hydrometeorological Applications: Severe Weather Precipitation Detection, Estimation, and Forecast. Advances in Meteorology, 2017, 2017, 1-2.	1.6	1
85	Xin'anjiang Nested Experimental Watershed (XAJ-NEW) for Understanding Multiscale Water Cycle: Scientific Objectives and Experimental Design. Engineering, 2021, , .	6.7	1
86	Advances in Remote Sensing and Modeling of Terrestrial Hydrometeorological Processes and Extremes. Advances in Meteorology, 2016, 2016, 1-3.	1.6	0
87	Inside Cover Image, Volume 3, Issue 6. Wiley Interdisciplinary Reviews: Water, 2016, 3, ii.	6.5	0
88	Evapotranspiration Mapping Utilizing Remote Sensing Data. , 2016, , 17-35.		0
89	An Advanced Distributed Hydrologic Framework. , 2016, , 127-138.		0